BIOLOGICAL CRYSTALLOGRAPHY
ISSN 1399-0047

Structural insights into *Aspergillus fumigatus* lectin specificity: AFL binding sites are functionally non-equivalent

Josef Houser,[a,b] Jan Komarek,[a,b] Gianluca Cioci,[c] Annabelle Varrot,[d] Anne Imberty[d] and Michaela Wimmerova[a,b,e]*

[a]Central European Institute of Technology, Masaryk University, Kamenice 5, 62500 Brno, Czech Republic, [b]National Centre for Biomolecular Research, Faculty of Science, Masaryk University, Kotlarska 2, 61137 Brno, Czech Republic, [c]Laboratoire d'Ingénierie des Systèmes Biologiques et des Procédés, Institut National des Sciences Appliquées, 31077 Toulouse CEDEX, France, [d]CERMAV–CNRS, UPR5301, affiliated with Université de Grenoble and ICMG, BP53, 38041 Grenoble CEDEX 9, France, and [e]Department of Biochemistry, Faculty of Science, Masaryk University, Kotlarska 2, 61137 Brno, Czech Republic. *Correspondence e-mail: michaw@chemi.muni.cz

Received 28 March 2014
Accepted 3 December 2014

Keywords: *Aspergillus fumigatus*; lectin; SPR; protein–saccharide complex; pathogen.

PDB references: AFL, apo, 4uou; complex with Lewis Y trisaccharide, 4d4u; complex with BGA, 4ah4; complex with αFuc(1–6)GlcNAc, 4agt; complex with L-Gal, 4d52; complex with βMeFuc, 4c1y; complex with a mixture of fucosylated monosaccharides, 4aha

Supporting information: this article has supporting information at journals.iucr.org/d

The *Aspergillus fumigatus* lectin AFL was recently described as a new member of the AAL lectin family. As a lectin from an opportunistic pathogen, it might play an important role in the interaction of the pathogen with the human host. A detailed study of structures of AFL complexed with several monosaccharides and oligosaccharides, including blood-group epitopes, was combined with affinity data from SPR and discussed in the context of previous findings. Its six binding sites are non-equivalent, and owing to minor differences in amino-acid composition they exhibit a marked difference in specific ligand recognition. AFL displays a high affinity in the micromolar range towards oligosaccharides which were detected in plants and also those bound on the human epithelia. All of these results indicate AFL to be a complex member of the lectin family and a challenging target for future medical research and, owing to its binding properties, a potentially useful tool in specific biotechnological applications.

1. Introduction

Saccharides play crucial roles not only in energy metabolism and cell structure, but also in signalling, protein modification and host–pathogen interactions. Various techniques for research in glycosciences have been developed to date (Mechref & Novotny, 2002; Meisen *et al.*, 2011; Tissot *et al.*, 2009), including mass spectrometry, immunological methods and the application of carbohydrate-specific hydrolases, among others. Lectins, which are ubiquitous carbohydrate-binding proteins, are also widely used for detecting and identifying glycans and glycosylation modifications. They are essential for the enzyme-linked lectin assay (ELLA), lectin blotting and sugar-specific labelling (Tissot *et al.*, 2009). Several structural lectin families have been described (http://www.glyco3d.cermav.cnrs.fr). Most of them share the phenomenon of multivalency, which is achieved by oligomerization and/or the presence of tandem repeats. One example that combines both approaches is the well known lectin from *Aleuria aurantia* (AAL). This protein was described in 1980 (Kochibe & Furukawa, 1980) and its structure was solved twenty years later (Fujihashi *et al.*, 2003; Wimmerova *et al.*, 2003). This lectin forms homodimers, with each monomer consisting of six tandem repeats folded into a six-bladed β-propeller. Each monomer bears five L-fucose-specific binding

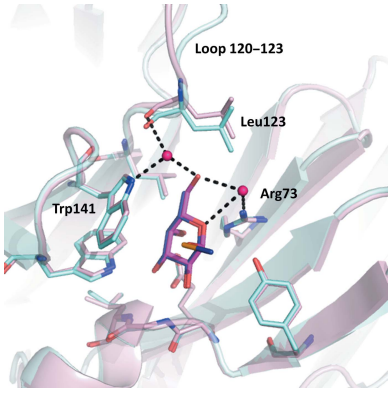

sites, sharing an overall binding pattern with the occurrence of hydrogen bonds to Arg and Glu/Gln residues, whereas a neighbouring Trp/Tyr residue mediates a CH–π interaction with the apolar surface of fucose. The five sites are similar but non-identical. The average affinity for fucose is in the micromolar range (Wimmerova *et al.*, 2003), but it has been proposed that some of the individual sites display much higher affinities (Olausson *et al.*, 2008). Several efforts have been made to understand the structure–function relationship at the binding-site level in order to correlate the composition of each binding site with its specificity and affinity (Amano *et al.*, 2004; Olausson *et al.*, 2011; Romano *et al.*, 2011). The studies of bacterial structural homologues (Audfray *et al.*, 2011; Kostlánová *et al.*, 2005) are beneficial but, as these lectins are much smaller and bear only two types of binding sites, they cannot completely explain the observed variability in AAL.

Owing to a rapid increase in the number of available gene sequences over the last decade, several homologues of the AAL protein have been identified, including lectins from *Aspergillus fumigatus* and *A. oryzae* (Ishida *et al.*, 2002). The crystal structure of AFL from *A. fumigatus* was recently solved as the first from a pathogenic mould (Houser *et al.*, 2013). AFL also has a dimeric arrangement of six-bladed β-propellers as in AAL, but it differs in the number of active binding sites, with six per monomer (Supplementary Fig. S1). The differences in the amino-acid composition of individual binding sites make this protein an ideal target for detailed studies focused on the relationship between the structure and the function of the lectin binding site. In addition, while *A. aurantia* is a harmless fungus, *A. fumigatus* acts as a worldwide allergen and is also a huge threat to immunocompromised patients, with a high mortality rate (Galimberti *et al.*, 2012). Recently, the presence of AFL in *Aspergillus* conidia was demonstrated (Houser *et al.*, 2013; Kuboi *et al.*, 2013), with a high probability of being localized at their surface. AFL recognizes fucose, which is widely present on oligosaccharide epitopes on human tissues (Becker & Lowe, 2003) and has been proved to be used by many pathogens for attachment (Imberty & Varrot, 2008). Furthermore, an immunostimulatory effect of AFL on human lung epithelial cells was observed. These findings make AFL a promising target for the diagnosis and/or treatment of aspergillosis. Better understanding of the binding properties of AFL may thus be useful in both biotechnology and medicine.

In this paper, we describe the crystal structures of several complexes of AFL with various human oligosaccharide receptors. Together with surface plasmon resonance measurements, the link between structure and binding properties in AAL family lectins is described.

2. Material and methods

2.1. Materials

Methyl-α,L-fucopyranoside was purchased from Interchim, Montluçon, France; L-galactose and blood group H type 2 trisaccharide were purchased from Dextra Laboratories Ltd, Reading, England. Other oligosaccharides were purchased from Carbohydrate Synthesis Ltd, Oxford, England. Basic chemicals were purchased from Sigma–Aldrich, St Louis, USA, Duchefa, Haarlem, The Netherlands and Applichem, Darmstadt, Germany.

2.2. Protein expression and purification

The AFL protein was produced as described previously (Houser *et al.*, 2013). Briefly, *Escherichia coli* BL21(DE3)Gold cells (Stratagene) bearing the pET29-*afl* vector were cultivated in standard low-salt LB medium with 50 µg ml^{-1} kanamycin. Induction with 1 m*M* isopropyl β-D-1-thiogalactopyranoside at 30°C for 3 h led to the overproduction of AFL. Harvested cells were disintegrated in 20 m*M* Tris–HCl pH 7.3 by sonication. AFL was isolated from the protein extract by affinity chromatography on mannose–agarose resin (Sigma–Aldrich) using isocratic elution. Fractions containing pure AFL protein were pooled, desalted by dialysis against ultrapure water and used for further studies or lyophilized.

2.3. Surface plasmon resonance

SPR measurements were performed using a Biacore 3000 instrument (GE Healthcare) at 25°C with running buffer [10 m*M* HEPES, 150 m*M* NaCl, 0.005% (*v*/*v*) Tween 20 pH 7.4] at a flow rate of 20 µl min^{-1}. To determine the binding preferences, the direct binding setup was chosen. The carboxymethyldextran surface of the CM5 chip was activated with EDC [*N*-ethyl-*N*-(3-dimethylaminopropyl)carbodiimide]/NHS (*N*-hydroxysuccinimide) solution using the manufacturer's standard protocol. Three different concentrations of AFL (1, 5 and 50 µg ml^{-1}) in 5 m*M* MES–NaOH pH 6.0 buffer were injected at a flow rate of 5 µl min^{-1} for 10 min into three flow channels. The relative responses of immobilized AFL were 800, 4500 and 11 900 response units, respectively. Finally, the sensor surface was blocked with 1 *M* ethanolamine. The blank channel was treated similarly except for the lectin injection. 80 µl of carbohydrate solutions with increasing concentrations in the running buffer were injected into the flow cells using the Inject mode. The equilibrium response (after subtracting the response of the reference surface) of each experiment was used to create analyte binding curves. Using the *Origin* 7.0 software (OriginLab), the data obtained for a particular ligand (all applicable runs on all channels) were simultaneously fitted, applying a common K_d value for all data sets. The one-site and two-site steady-state affinity models were used based on the equations $R = R_{max}c(\text{ligand})/[K_d + c(\text{ligand})]$ and $R = R_{max1}c(\text{ligand})/[K_{d1} + c(\text{ligand})] + R_{max2}c(\text{ligand})/[K_{d2} + c(\text{ligand})]$, respectively, where R is the detector response, R_{max} is the maximal response, K_d is the dissociation constant and c(ligand) is the actual concentration of injected ligand. The R_{max1}:R_{max2} ratio in the two-site model was not restricted in order to not influence the values of K_{d1} and K_{d2}. Depending on the channel, the experimental R_{max} values typically reached 10–40% of the theoretical R_{max}.

2.4. Crystallization and data collection

Lyophilized protein was dissolved in ultrapure water and subsequently used in crystallization experiments using the hanging-drop method. The initial crystallization conditions were the same as described previously (Houser *et al.*, 2013); the conditions were optimized for each ligand used. The final crystals were obtained from a set of drops under the following conditions: 2 µl precipitant (200 m*M* $CaCl_2$, 25% PEG 4K, 100 m*M* Tris pH 8.5) was mixed with 2 µl protein solution consisting of 7–15 mg ml^{-1} AFL and a dissolved ligand (Supplementary Fig. S2). The ligand concentrations used were as follows: blood group A trisaccharide (BGA; 2 m*M*), Lewis Y tetrasaccharide (Le^Y; 1 m*M*), α,L-fucosyl(1–6)-*N*-acetyl-D-glucosamine (1 m*M*), L-galactose (L-Gal; 1 m*M*), methyl-β,L-fucoside (1 m*M*) or an equimolar mixture (1 m*M* each) of αFuc(1–2)Gal, αFuc(1–3)GlcNAc, αFuc(1–4)GlcNAc and αFuc(1–6)GlcNAc. Ligand-free AFL was treated in the same way but omitting the addition of the ligand. The plates were incubated at 17°C until crystals formed.

Crystals were cryocooled at 100 K after soaking for the shortest possible time in reservoir solution supplemented with 15%(*v*/*v*) glycerol (AFL–BGA), 20%(*v*/*v*) glycerol [AFL–Le^Y, AFL–Fucα(1–6)GlcNAc and AFL–βMeFuc] or 40%(*v*/*v*) PEG 400 (ligand-free AFL, AFL–L-Gal and AFL–disaccharide mixture). The X-ray diffraction experiments were performed on beamlines 14.1 (ligand-free AFL) and 14.2 (AFL–βMeFuc) at BESSY II, Berlin, Germany (Mueller *et al.*, 2012) or on the ID23-1 or ID23-2 beamlines at the European Synchrotron Radiation Facility (ESRF), Grenoble, France (all other complexes; Nurizzo *et al.*, 2006).

2.5. Structure determination

The diffraction images collected were processed using *iMosflm* v.7 (Leslie & Powell, 2007; Battye *et al.*, 2011) or *XDS* (Kabsch, 2010) and were converted to structure factors using the *CCP*4 program package v.6.1 (Winn *et al.*, 2011), with 5% of the data reserved for $R_{\rm free}$ calculation. The structures of the AFL complexes were determined using the molecular-replacement method with *MOLREP* v.10.2 (Vagin & Teplyakov, 2010) or *Phaser* v.2.5 (McCoy *et al.*, 2007), respectively, using the structure of AFL–MeSeFuc (PDB entry 4agi; Houser *et al.*, 2013) without the ligands as the starting model. Refinement of the molecule was performed using *REFMAC5* (Murshudov *et al.*, 2011) alternated with manual model building in *Coot* v.0.7 (Emsley *et al.*, 2010). Sugar residues and other compounds that were present were placed manually using *Coot*. Water molecules were added by *Coot* and checked manually. The addition of alternative conformations, where necessary, resulted in final structures that were validated using the *ADIT* (http://rcsb.pdb.org) and *MolProbity* (Chen *et al.*, 2010; http://molprobity.biochem.duke.edu) validation servers and were deposited in the PDB as entries 4d4u (AFL–Le^Y), 4ah4 (AFL–BGA), 4agt [AFL–αFuc(1–6)GlcNAc], 4d52 (AFL–L-Gal), 4c1y (AFL–βMeFuc) and 4aha [AFL with an equimolar mixture of αFuc(1–2)Gal, αFuc(1–3)GlcNAc, αFuc(1–4)GlcNAc and αFuc(1–6)GlcNAc].

2.6. Analytical ultracentrifugation

Sedimentation analysis was performed using a ProteomeLab XL-A analytical ultracentrifuge (Beckman Coulter) equipped with an An-60 Ti rotor. Before analysis, purified AFL was brought into the experimental buffer by dialysis and the dialysate was used as an optical reference. Sedimentation-velocity experiments were performed with 0.2 mg ml^{-1} AFL. Three different buffers were tested for pH dependence: (i) 20 m*M* sodium citrate buffer, 150 m*M* NaCl pH 4.0, (ii) 20 m*M* Tris–HCl, 150 m*M* NaCl pH 7.3 and (iii) 20 m*M* sodium carbonate buffer, 150 m*M* NaCl pH 10.0. The influence of the ionic strength was analyzed by varying the concentration of NaCl (0–1000 m*M*) in 20 m*M* Tris–HCl buffer pH 7.3 buffer. Sedimentation-velocity experiments were conducted in a standard double-sector centrepiece cell loaded with 420 µl protein sample and 430 µl reference solution. Data were collected using absorbance optics at 25°C and a rotor speed of 40 000 rev min^{-1}. Scans were performed at 280 nm at 8 min intervals and 0.003 cm spatial resolution in continuous scan mode. The partial specific volumes of the protein together with the solvent density and viscosity were calculated from the amino-acid sequence and buffer composition, respectively, using *SEDNTERP* (http://bitcwiki.sr.unh.edu). Sedimentation profiles were analyzed with *SEDFIT* v.13.0 (Schuck, 2000). A continuous size-distribution model for non-interacting discrete species was used to provide a distribution of apparent sedimentation coefficients.

3. Results

3.1. AFL–saccharide interaction

3.1.1. Surface plasmon resonance. The SPR technique was employed in order to determine the binding affinities of AFL towards various biologically relevant saccharides. Immobilization of the protein on the chip surface was chosen to avoid the complex interpretation of interactions with a multivalent saccharide-modified surface. The data were processed using *Origin* 7.0. Using the one-site model, the dissociation constants towards fucose and all fucosylated compounds (Table 1) were rather similar and were close to 0.1 m*M*. The affinity for L-galactose was lower ($K_{\rm d}$ = 0.78 m*M*), indicating the importance of the C6 methyl group of L-fucose. However, as displayed in Supplementary Fig. S3, the fit between the experimental data and the one-site model of binding is not always good, and a more complex model could be envisaged. In theory, a six-binding sites model could be used, but this would result in a very large number of variables, which could lead to overfitting problems. Therefore, the use of a two-sites model is rationalized by the occurrence of two sets of binding sites, depending on the presence of a Trp or a Tyr residue (Houser *et al.*, 2013), as previously described for the *A. aurantia* lectin (Amano *et al.*, 2004). This approach usually results in a better fit between the experimental data and the model, as displayed in Supplementary Fig. S3, therefore validating the proposition of a second set of binding sites with higher affinities (a $K_{\rm d}$ of a few micromolar) for fucosylated

Table 1
Apparent K_d values for the interaction of biologically important saccharides with AFL using SPR measurements.

Values are given with standard deviations based on measurements on three independent channels with different amounts of immobilized AFL.

Ligand	K_d (one site) (μ*M*)	K_{d1} (two sites) (μ*M*)	K_{d2} (two sites) (μ*M*)
Fuc	209 ± 15	408 ± 40	91.9 ± 32.8
αMeFuc	120 ± 8	958 ± 189	83.0 ± 4.9
βMeFuc	251 ± 29	†	†
L-Gal	775 ± 71	†	†
αFuc(1–2)Gal	82.3 ± 5.2	220 ± 39	14.2 ± 4.3
αFuc(1–3)GlcNAc	71.7 ± 5.7	278 ± 19	7.28 ± 0.91
αFuc(1–4)GlcNAc	63.3 ± 4.9	202 ± 8	4.10 ± 0.42
αFuc(1–6)GlcNAc	84.0 ± 4.7	206 ± 18	15.0 ± 2.1
αFuc(1–2)[αGalNAc(1–3)]Gal, blood group A trisaccharide	68.0 ± 5.9	183 ± 47	11.5 ± 4.5
αFuc(1–2)[αGal(1–3)]Gal, blood group B trisaccharide	61.7 ± 4.7	181 ± 28	10.3 ± 2.3
αFuc(1–2)βGal(1–4)GlcNAc, blood group H type 2 trisaccharide	68.3 ± 7.8	192 ± 34	4.38 ± 1.68
αFuc(1–4)[βGal(1–3)]GlcNAc, Lewis A trisaccharide	101 ± 13	442 ± 79‡	8.24 ± 1.90
αFuc(1–3)[βGal(1–4)]GlcNAc, Lewis X trisaccharide	172 ± 11	246 ± 9	1.80 ± 0.53
αFuc(1–2)βGal(1–3)[αFuc(1–4)]GlcNAc, Lewis B tetrasaccharide	131 ± 7	249 ± 59	26.6 ± 13.3
αFuc(1–2)βGal(1–4)[αFuc(1–3)]GlcNAc, Lewis Y tetrasaccharide	75.8 ± 3.1	113 ± 6	3.85 ± 1.07

† Values not determined. Two-site models for βMeFuc and L-Gal were unable to reach a meaningful fit. ‡ The K_d value is less precise since it lies at the edge of the range of concentrations tested.

compounds. The ratio between higher and lower affinity sites was usually close to 1:5 or 2:4, which suggests an even more complex behaviour of the system. Only for L-Gal and βMeFuc did the one-site model fit the data better than the two-sites model.

AFL displays a slight preference for the α-anomeric fucoside, but the β-fucoside is also recognized. L-Gal does not bind so efficiently, confirming the hydrophobic interaction owing to the fucose methyl group close to the semi-conserved Leu/Ile/Met residues. The highest affinity is for the Lewis X and Lewis Y epitopes, but it could be concluded that AFL has a general fucose specificity, since all tested human fucosylated oligosaccharides were efficiently bound by the lectin.

3.2. Structural studies

3.2.1. Structure determination. The structures of sugar-free AFL and AFL co-crystallized with various ligands were solved by molecular replacement using the protein coordinates of chain *A* of the AFL–selenofucoside structure (PDB entry 4agi) as the search model. Ligand-free AFL crystallized in space group $P2_1$ and the sugar complexes crystallized in space groups $P1$, $P2_1$ or $P2_12_12_1$ (see Table 2 for details).

In all structures, the AFL protein adopts the six-bladed β-propeller fold previously determined for the MeSeFuc complex. No significant variations of the backbone conformation were observed between the chains within a particular structure or between the different structures, with r.m.s.d.s varying from 0.10 to 0.33 Å when compared with the previously published structure (Houser *et al.*, 2013). Two single-point mutations L20S and R111C previously reported to be natural variations were clearly detected in all of the present structures. Some cysteine residues in the BGA, Le^Y and L-Gal complexes were found to be oxidized, since no DTT or other reducing agents were used during crystallization. Neither the cysteines nor their oxidized forms participate in ligand binding. In some complexes additional ions (sodium, chloride, zinc) and organic molecules (PEG) originating from the crystallization conditions were detected. They also did not affect the ligand binding or the oligomeric state of the protein.

3.2.2. Oligomeric state. AFL is a dimeric protein in solution and crystallizes as a dimer in all complexes, similarly to the previously analyzed complex with methyl seleno-α,L-fucopyranoside (Houser *et al.*, 2013). In all structures, the protein associates using the same dimeric interface, which involves mainly the side chains of the Gln7, Tyr109, Asn134, Asn238 and Gln262 residues and the backbone of the Asn235, Ser236 and Gly263 residues. One or two dimers are observed in the asymmetric unit depending on the space group (Table 2). Comparison of the *AB* dimers in the different crystal structures results in r.m.s.d. values of 0.20–0.24 Å. Compared with the dimer formed by its structural homologue AAL, the AFL lectin exhibits significant differences. The amino acids involved in the dimeric interface either differ in their sequence or in their position, and this leads to changes in the respective orientation of the two monomers in both dimers (Supplementary Figs. S4 and S5).

The existence of dimeric AFL in solution at neutral pH was originally determined by analytical ultracentrifugation (Houser *et al.*, 2013). Additional AUC experiments at various pH values were performed to determine the stability of the AFL dimer in solution (Supplementary Fig. S6). An acidic pH of 4, which has been reported to affect the conidia binding of *A. fumigatus* (Tiralongo *et al.*, 2009), does not affect the oligomeric form at all; hence, there is probably no link between the AFL oligomeric state and inhibition of conidia binding. However, a shift to pH 10, which is beyond the typical pH for *A. fumigatus* growth (pH 2.1–8.8; Kwon-Chung & Sugui, 2013), causes a dissociation of 7% of AFL into monomers. The protein dimer was stable at neutral pH with various concentrations of NaCl (150–1000 m*M*; data not shown), which corresponds to the results published previously for a lower ionic strength of below 300 m*M* NaCl (Houser *et al.*, 2013).

Table 2
Data-collection and refinement statistics.

Values in parentheses are for the outer shell.

Ligand	L-Gal	βMeFuc	Fucα(1–6)GlcNAc	Disaccharide mixture†	BGA	Le^Y	None
PDB code	4d52	4c1y	4agt	4aha	4ah4	4d4u	4uou
Data-collection statistics							
Beamline	ID23-1, ESRF	14.2, BESSY II	ID23-2, ESRF	ID23-2, ESRF	ID23-1, ESRF	ID23-2, ESRF	14.1, BESSY II
Wavelength (Å)	0.9763	0.9184	0.8726	0.8726	0.9795	0.8726	0.9184
Space group	$P2_1$	$P2_12_12_1$	$P2_1$	$P2_1$	$P1$	$P1$	$P2_1$
a (Å)	80.03	71.21	47.41	45.73	46.42	47.32	47.63
b (Å)	70.44	90.34	88.35	88.38	47.44	47.53	140.22
c (Å)	117.80	189.17	79.78	78.58	80.09	77.36	78.79
α (°)	90.00	90.00	90.00	90.00	103.61	96.81	90.00
β (°)	108.34	90.00	102.95	99.63	91.96	100.24	92.15
γ (°)	90.00	90.00	90.00	90.00	113.08	113.61	90.00
No. of monomers in asymmetric unit	4	4	2	2	2	2	4
Resolution range (Å)	34.44–1.75 (1.85–1.75)	48.14–2.23 (2.35–2.23)	38.87–2.00 (2.11–2.00)	36.41–2.20 (2.32–2.20)	42.03–1.75 (1.84–1.75)	42.01–1.99 (2.10–1.99)	78.74–2.40 (2.53–2.40)
Total No. of reflections	448327 (63804)	168544 (16725)	102700 (11494)	104127 (15841)	138182 (18326)	122864 (15105)	163605 (24505)
No. of unique reflections	121067 (8051)	56964 (5173)	38241 (4925)	27431 (1286)	57394 (7620)	39131 (5255)	40256 (5854)
Completeness (%)	97.3 (95.5)	99.0 (97.8)	88.2 (80.0)	87.5 (71.8)	94.1 (85.3)	96.1 (88.9)	99.7 (99.5)
Multiplicity	3.7 (3.7)	8.2 (3.2)	2.4 (2.4)	2.1 (2.1)	2.4 (2.4)	3.1 (2.9)	4.1 (4.2)
$\langle I/\sigma(I)\rangle$	12.0 (3.2)	6.1 (1.5)	7.1 (2.4)	7.1 (2.6)	14.3 (2.5)	11.6 (2.5)	12.9 (8.7)
R_{merge}	0.082 (0.390)	0.130 (0.350)	0.110 (0.440)	0.120 (0.380)	0.050 (0.353)	0.077 (0.379)	0.064 (0.108)
$CC_{1/2}$	0.996 (0.879)	0.996 (0.563)	0.985 (0.567)	0.983 (0.750)	0.999 (0.887)	0.997 (0.892)	0.996 (0.988)
Wilson B factor (Å^2)	13.9	30.8	15.9	16.7	15.8	20.8	8.2
Refinement statistics							
No. of amino acids	4 × 314	4 × 314	2 × 314	2 × 314	2 × 314	2 × 314	4 × 314
No. of protein atoms							
Chain A	2449	2439	2443	2444	2454	2438	2437
Chain B	2455	2443	2440	2451	2445	2455	2439
Chain C	2439	2434					2437
Chain D	2446	2438					2442
No. of solvent atoms	1070	137	423	443	556	412	526
No. of ligand atoms	341	201	175	203	357	344	14
Resolution limits (Å)	34.44–1.76 (1.80–1.76)	47.29–2.23 (2.29–2.23)	38.87–2.00 (2.05–2.00)	36.41–2.20 (2.26–2.20)	42.03–1.75 (1.80–1.75)	42.01–1.99 (2.04–1.99)	78.74–2.40 (2.46–2.40)
No. of reflections in working set	114970 (8319)	56864 (4095)	36310 (2342)	26054 (3722)	54494 (3283)	37163 (2343)	38050 (2828)
No. of reflections in test set	6078 (436)	2993 (215)	2172 (110)	2472 (198)	2897 (174)	1967 (119)	2008 (136)
Final R_{cryst} (%)	15.3 (25.6)	24.2 (35.1)	17.2 (28.8)	16.5 (36.4)	16.8 (28.1)	16.9 (30.3)	21.7 (19.7)
Final R_{free} (%)	17.8 (28.2)	31.3 (42.4)	21.2 (29.2)	21.2 (41.7)	21.1 (30.0)	22.0 (33.1)	27.9 (29.8)
Mean B factor (Å^2)	17.27	26.96	16.07	15.28	18.95	24.81	11.30
R.m.s. deviations							
Bonds (Å)	0.010	0.012	0.011	0.016	0.012	0.009	0.014
Angles (°)	1.455	1.495	1.447	1.727	1.419	1.412	1.610
Planar groups (Å)	0.007	0.007	0.007	0.008	0.006	0.005	0.007
Chiral volumes (Å^3)	0.088	0.085	0.090	0.101	0.080	0.079	0.088
Ramachandran plot							
Most favoured (%)	97.5	94.1	97.5	97.0	97.9	97.3	95.3
Allowed (%)	2.2	5.4	2.2	2.9	1.8	2.4	4.3
Outliers (%)	0.3	0.5	0.3	0.1	0.3	0.3	0.4

† An equimolar mixture of αFuc(1–2)Gal, αFuc(1–3)GlcNAc, αFuc(1–4)GlcNAc and αFuc(1–6)GlcNAc disaccharides was used for crystallization.

3.2.3. AFL binding sites. AFL contains six binding sites per monomer, each located between two adjacent blades (Houser *et al.*, 2013). According to the nomenclature used previously, site 1 is located between blades I and II and so on, finishing with site 6 between blade VI and blade I. Clear electron density corresponding to AFL ligands was observed in all structures, sometimes in all binding sites and sometimes in only some of them (Supplementary Fig. S7). The binding sites in all protein subunits of particular complex display similar behaviour unless stated otherwise.

The molecular structure of AFL co-crystallized with different oligosaccharides revealed only minor changes in side-chain positions. The binding mode for the fucosyl part of the oligosaccharides is the same as that observed with MeSeFuc (Supplementary Fig. S1). Only a minor shift of the fucose position is observed in some complexes with larger oligosaccharides. A summary of the ligands detected in the binding sites of each complex is given in Table 3. In several cases, only the fucose moiety could be identified in the electron density, which indicates probable flexibility of the remaining part of the oligosaccharide. The AFL structure without any ligand reveals higher flexibility of particular amino-acid side chains (especially Arg25 in site 1, Trp141 in site 2 and Trp299 in site 5), while the overall shape of the binding site is retained (Supplementary Fig. S8).

Table 3
Ligands coordinated in the individual binding sites of AFL crystal structures.

Only the clearly defined parts of a saccharide are listed. Saccharide units directly bound to protein are in bold, those bound *via* a water molecule are underlined and ligands stabilized by crystal-packing interactions are in italics. In all cases the interaction cutoff was set to 3.6 Å.

Ligand		L-Gal	L-Gal†	βMeFuc	βMeFuc†	Fucα(1–6)GlcNAc	Fuc mixture‡	BGA	Le^Y
Chain *A*	Site 1	**L-Gal**	**L-Gal**	***β*MeFuc**	***β*MeFuc**	**Fuc**	**Fuc**	**αFuc**1–2(α***GalNAc***1–3)**Gal**	**αFuc**1–2β**Gal**1–4**GlcNAc**
	Site 2	**L-Gal**	**L-Gal**	**Glycerol**	—	**αFuc**1–6***GlcNAc***	αFuc1–4GlcNAc	**αFuc**1–2(α*GalNAc*1–3)Gal	**αFuc**β1–2Gal1–4GlcNAc
	Site 3	***L-Gal***	***L-Gal***	**βMeFuc**	***β*MeFuc**	**Fuc**	**Fuc**	**Fuc**	αFuc1–2β**Gal**1–4(**αFuc**1–3)*GlcNAc*
	Site 4	**PEG**	**PEG**	**Glycerol**	—	**Fuc**	**Fuc**	**αFuc**1–2(α*GalNAc*1–3)Gal	**Glycerol**
	Site 5	**PEG**	**PEG**	**Glycerol**	***β*MeFuc**	**Fuc**	**Fuc**	**αFuc**1–2(α**GalNAc**1–3)Gal	**Fuc**
	Site 6	**L-Gal**	**L-Gal**	**βMeFuc**	***β*MeFuc**	**Fuc**	**Fuc**	**αFuc**1–2(α*GalNAc*1–3)Gal	**αFuc**1–2β**Gal**1–4(**αFuc**1–3)**GlcNAc**
Chain *B*	Site 1	**L-Gal**	**L-Gal**	**βMeFuc**	—	**Fuc**	**αFuc**1–4***GlcNAc***	**αFuc**1–2(α**GalNAc**1–3)**Gal**	**αFuc**1–2β*Gal*1–4**GlcNAc**
	Site 2	**L-Gal**	**L-Gal**	***Glycerol***	**Glycerol**	**Fuc**	**αFuc**1–4*GlcNAc*	**Fuc**	**αFuc**1–2β*Gal*1–4*GlcNAc*
	Site 3	**L-Gal**	**L-Gal**	**βMeFuc**	***β*MeFuc**	**Fuc**	**Fuc**	**Fuc**	αFuc1–2β**Gal**1–4(**αFuc**1–3)**GlcNAc**
	Site 4	**PEG**	**PEG**	—	—	**Fuc**	**αFuc**1–4**GlcNAc**	**αFuc**1–2(α**GalNAc**1–3)Gal	**Glycerol**
	Site 5	**PEG**	**PEG**	**Glycerol**	—	**αFuc**1–6*GlcNAc*	**Fuc**	**αFuc**1–2(α**GalNAc**1–3)Gal	**Fuc**
	Site 6	**L-Gal**	**L-Gal**	***β*MeFuc**	***β*MeFuc**	**Fuc**	**Fuc**	**αFuc**1–2(α**GalNAc**1–3)**Gal**	**αFuc**1–2*Gal*

† Ligands from chains *C* and *D* are shown instead of those from chains *A* and *B*, respectively. ‡ An equimolar mixture of αFuc(1–2)Gal, αFuc(1–3)GlcNAc, αFuc(1–4)GlcNAc and αFuc(1–6)GlcNAc disaccharides was used for crystallization.

All six binding sites share a typical binding motif. Conserved Arg and Glu/Gln residues establish polar interactions with the O3, O4 and O5 hydroxyls of the bound fucose, and a Trp/Tyr residue mediates a CH–π interaction with the apolar surface of fucose (C3, C4 and C5). Additional hydrogen bonds may be formed between the saccharide and the other residues. These interactions are different for each binding site and for each ligand. Additional hydrophobic interactions are mainly present between C6 of the fucose and nonpolar amino acids in the binding site, including the semi-conserved Leu/Ile/Met in the pocket at the bottom of the site.

3.2.4. AFL–L-Gal complex. AFL was co-crystallized with L-Gal in order to determine the role of the L-Fuc methyl group in sugar binding. The structure revealed electron density corresponding to L-Gal in four out of six binding sites for each monomer (Table 3). In sites 3 and 6 and for three out of four chains in site 1, both α- and β-anomers were detected. Site 2 seems to be specific for α,L-Gal.

The orientation of L-Gal is identical to that observed for L-Fuc (Fig. 1). The additional OH group points outside the hydrophobic pocket and is stabilized by two bridging water molecules, mainly towards the side chains of the conserved amino acids Arg and Tyr/Trp. In site 1, it is further stabilized by a hydrogen bond to the main-chain O atom of Leu69. The position of the amino-acid side chains in the vicinity of the ligand are the same as in the complex with MeSeFuc. Only the Leu123 side chain changes its conformation slightly, so that it does not clash with the O6 hydroxyl of L-Gal. However, the displacement of the 120–123 loop observed in chains *A* and *D* is probably owing to intermonomeric interactions in the crystal. Since no other structural changes were observed, the unfavourable accommodation of O6 of L-Gal in the hydrophobic pocket in the binding site together with the restriction of O6 rotational movement (entropic penalty) are probable causes of its lower affinity towards L-Gal as determined by SPR.

3.2.5. AFL–βMeFuc complex. AFL is able to recognize βMeFuc, as shown by a glycan array (Houser *et al.*, 2013) and by SPR. To more deeply understand the observed difference between the binding of α- and β-linked fucosides, the structure of the AFL–βMeFuc complex was solved. Electron density corresponding to the ligand was detected in all four monomers in the asymmetric unit for sites 3 and 6 and in three out of four monomers in site 1 (Table 3). βMeFuc was also localized in site 5 of chain *C*, where it is stabilized by intermonomeric interactions enabled by crystal packing. All other sites remained unoccupied or density for glycerol (the cryoprotectant) was detected.

The sugar ligand is stabilized by a Tyr-mediated stacking interaction in sites 1, 3 and 6. This corresponds to a lower

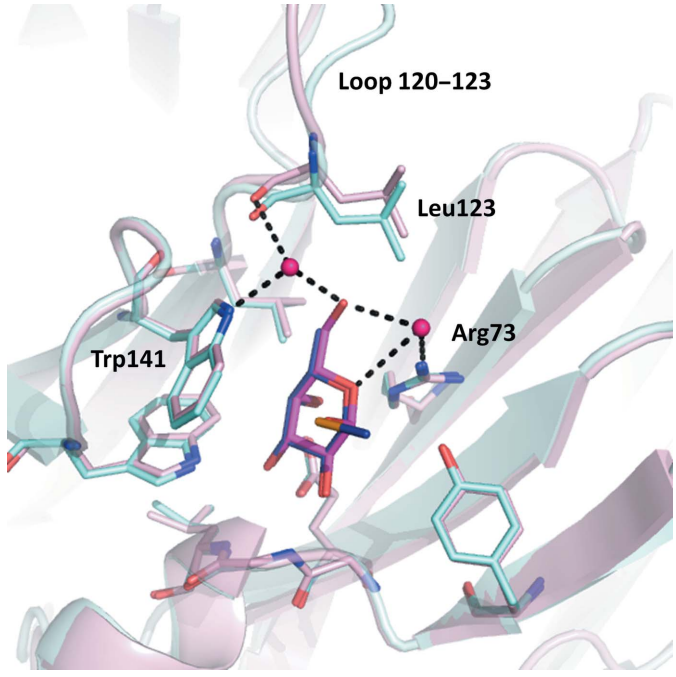

Figure 1
Comparison of AFL site 2 in chain *A* of the L-Gal complex (pink) with that in the MeSeFuc complex (cyan). L-Gal (C atoms in magenta) adopts the same orientation as MeSeFuc (C atoms in blue) and is stabilized by two conserved water molecules (shown as spheres). The minor shift in the position of the Leu123 side chain and the different orientation of loop 120–123 can be seen at the top of the figure.

affinity as determined by SPR, where the one-site model also fits better than the two-site model. The position of βMeFuc in the binding sites is identical to that in the αMeSeFuc complex, with no additional interaction between the methoxy group and the protein. Since there would be no steric conflict between the βMeFuc methoxy group and the stacking Trp residue, it is possible that the side chains of Tyr95 and Tyr199 on the opposite side of the binding pocket cause the absence of βMeFuc in sites 2 and 4, respectively (Fig. 2). The residues in the equivalent positions of occupied binding sites, Leu39 (site 1), Met140 (site 3) and Val298 (site 6), do not interfere with βMeFuc, thus enabling its binding.

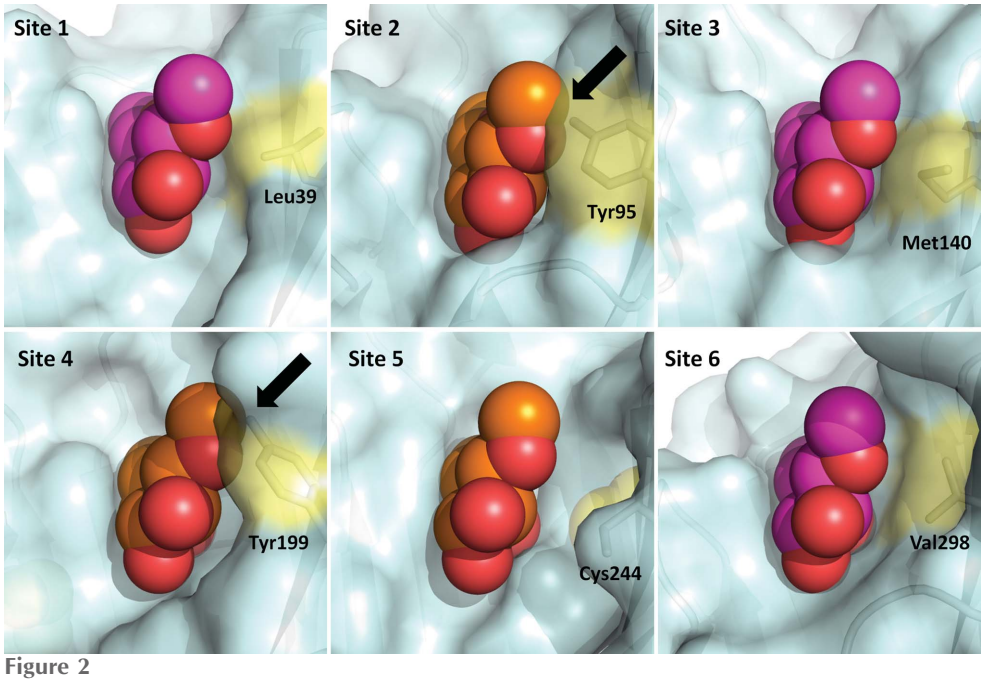

Figure 2
AFL binding sites with βMeFuc (magenta). In sites 1, 3 and 6 the βMeFuc molecule crystallographically assigned in chain *A* of the AFL–βMeFuc complex structure is shown (magenta). In sites 2, 4 and 5, where no βMeFuc was detected, the shown βMeFuc (orange) was superposed according to the MeSeFuc molecule from the AFL–MeSeFuc complex (PDB entry 4agi). Possible steric conflicts are indicated by black arrows. Tyr95 and Tyr199 that would probably collide with βMeFuc in sites 2 and 4, respectively, and the corresponding amino acids in other sites are highlighted in yellow.

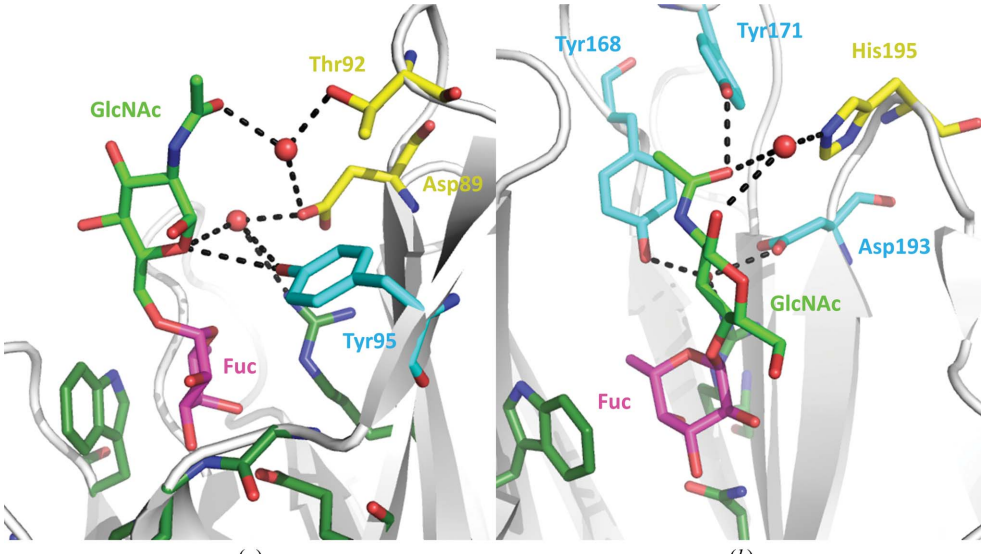

(*a*) (*b*)

Figure 3
(*a*) Binding site 2 of chain *A* of the AFL–Fucα(1–6)GlcNAc complex. (*b*) Fucα(1–4)GlcNAc in binding site 4 of chain *B* of the AFL complex crystallized with a mixture of fucosylated disaccharides. Hydrogen bonds linking a GlcNAc moiety to the protein side chains are highlighted in both panels. Colour code: fucose, magenta; GlcNAc, green. For sugar-binding amino acids: dark green, fucose-binding residues; cyan, direct interaction with GlcNAc; yellow, water-mediated interaction with GlcNAc.

3.2.6. AFL–disaccharide complexes. The disaccharide αFuc(1–6)GlcNAc, which corresponds to core fucosylation on N-glycans, was co-crystallized with the lectin, and electron density for the fucosyl part was clearly seen in all six binding sites. Owing to the inherent flexibility of the 1–6 linkage, the GlcNAc moiety was only visible in site 2 of chain *A* and site 5 of chain *B*, when stabilized by interactions with a neighbouring molecule owing to crystal packing. Only one direct interaction between GlcNAc and protein was observed, linking the O5 atom of GlcNAc to Tyr95 OH in site 2 of chain *A* (Fig. 3*a*). Additional interactions are mediated by water bridges connecting O5 to the side chains of Arg73, Asp89 and Tyr95 and O7 to those of Asp89 and Thr92. In site 5 of chain *B*, the only interaction with the protein chain is mediated by a water molecule connecting O1 of αGlcNAc and Trp299 NE1. Some other interactions, either direct or mediated by the solvent, are observed with symmetric molecules, especially at the level of the *N*-acetyl group. Hence, each AFL binding site is able to recognize fucose by the 1–6 linkage, but probably owing to the flexibility of this linkage the GlcNAc residue mostly moves freely in the solvent and does not provide additional stability to the interaction.

In order to determine the preferences of particular binding sites, AFL was also co-crystallized with an equimolar mixture of four fucosylated disaccharides: αFuc(1–2)Gal, αFuc(1–3)GlcNAc,

αFuc(1–4)GlcNAc and αFuc(1–6)GlcNAc. In all six binding sites in both the *A* and *B* chains, electron density for the fucose moiety was clearly detected. In site 2 of chain *A* and sites 1, 2 and 4 of chain *B* the density was clear enough to assign the second saccharide unit (Table 3). In all these cases, only αFuc(1–4)GlcNAc was observed. In addition to the conserved interactions in the fucose binding site, GlcNAc is stabilized by direct hydrogen bonds to Tyr88 OH (site 1) or Tyr168 OH, Tyr171 OH and Asp193 OD2 (site 4) and by water-mediated bridges (Fig. 3*b*). In the other sites electron density for the second saccharide is not clear, indicating either large flexibility of the disaccharide linkage [probable for αFuc(1–6)GlcNAc] or statistical disorder (different oligosaccharides present in one binding site).

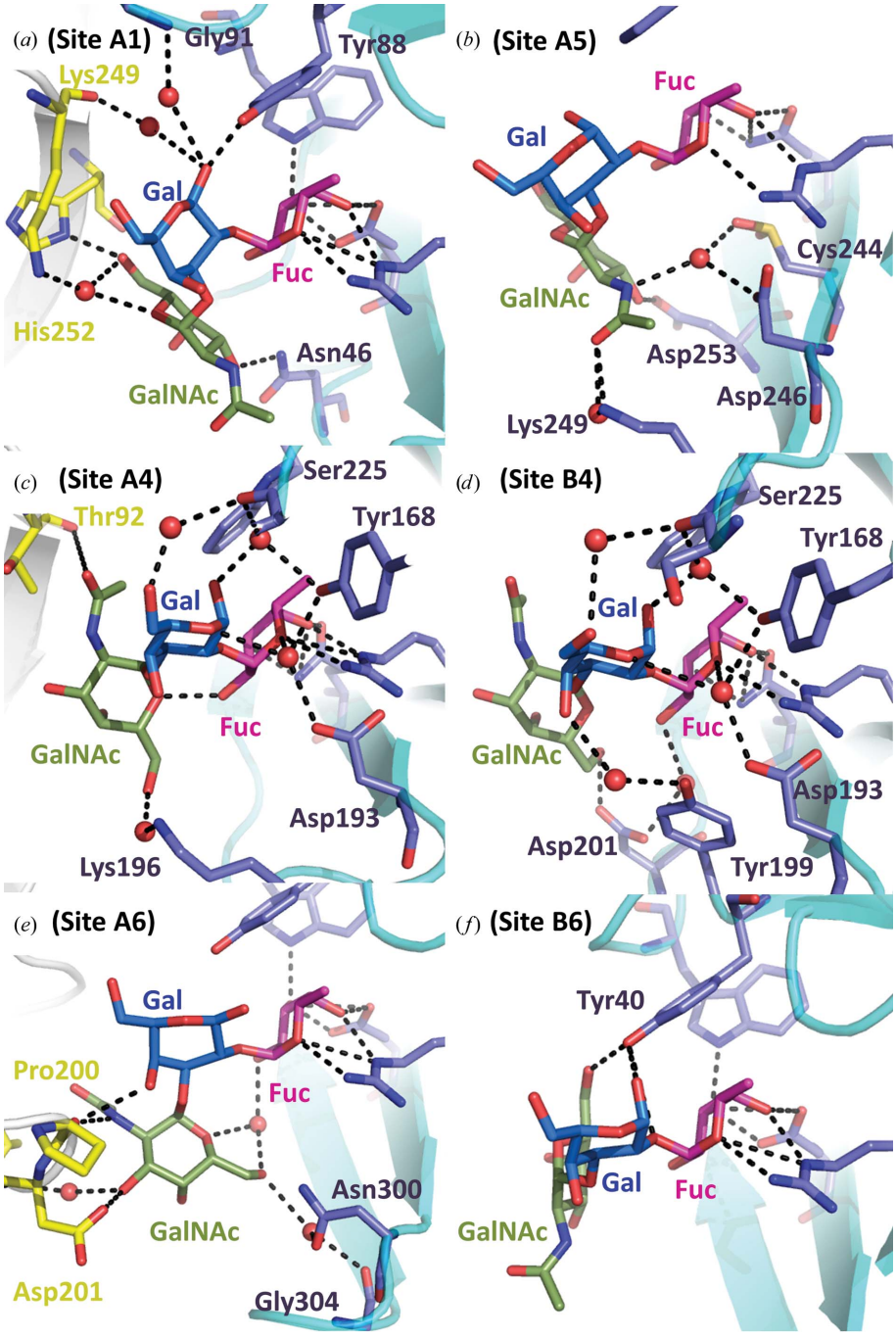

Figure 4
BGA trisaccharide complex with AFL. Sites are labelled according to chain and site number in each panel. Interacting residues are labelled when stabilizing a Gal or GalNAc moiety directly or *via* a water bridge. Interacting residues from a neighbouring monomer in the crystal (shown in yellow) cause different oligosaccharide conformations in site 6 of chain *A* and chain *B*. Colour code: fucose, magenta; galactose, blue; GalNAc, olive. Bridging water molecules are represented as red spheres and hydrogen bonds between saccharide and protein or water molecules as black dashed lines.

3.2.7. AFL–BGA complex. Electron density for the whole blood group A trisaccharide was observed in all sites except for site 3 of chain *A* and sites 2 and 3 of chain *B* (Supplementary Fig. S7*d*). The density was not clear in all parts, yet was sufficient to analyze the main protein–ligand interactions. In addition to the conserved interaction with fucose, Tyr40 (in chain *B*; Fig. 4*f*) and Tyr88 (in both chains *A* and *B*; Fig. 4*a*) mediate hydrogen bonds to the Gal moiety in sites 6 and 1, respectively. The missing interaction of the Gal moiety with Tyr40 in site 6 of chain *A* (Fig. 4*e*) is affected by intermolecular interactions, as described below. Additional interactions occurred between GalNAc and the Asp201 side chain (site 4) in chain *B* (Fig. 4*d*) or the Asp253 side chain (site 5) in chain *A* (Fig. 4*b*). The ligands in sites 1, 2, 4 and 6 of chain *A* are further stabilized by intermolecular interactions in the crystal; however, in sites 1 and 2 this does not seem to markedly influence the oligosaccharide conformation when comparing it with the computed theoretical energy minimum for the free ligand (Imberty *et al.*, 1995; Fig. 5). The greatest difference is exhibited by the GalNAcα(1–3)Gal linkage for the ligand in site 4 of both chains (Fig. 5*b*), which could be owing to a stabilizing interaction between GalNAc OH6 and Asp201 OD2 (chain *B*; Fig. 4*d*), a water bridge to Lys196 NZ or crystal interactions (chain *A*; Fig. 4*c*). For site 6, the interactions of the ligand with the neighbouring protein monomer in the crystal are of importance. In chain *B*, the Gal and GalNAc moiety is linked to Tyr40 OH. In chain *A*, the ligand prefers to coordinate to Pro200 O and Asp201 OD2 of the neighbouring protein molecule in the crystal. This leads to a conformational change of the trisaccharide (Figs. 4*e*, 4*f* and 5*b*). Additional stabilizing interactions result

in small differences between the observed conformations of the ligand in each particular binding site of the protein; however, they generally correspond to the conformations of the particular sugar linkages in PDB-deposited structures.

3.2.8. AFL–Le^{Y} complex. The Lewis Y tetrasaccharide (Le^{Y}), containing one L-fucose bound by an α-1,2 linkage and one bound by an α-1,3 linkage, was determined to be the epitope best recognized in a glycan-array experiment using the biologically relevant oligosaccharides (Houser *et al.*, 2013). Clear electron density for the complete Le^{Y} was observed in binding site 3 of both chains and in site 6 of chain *A*. For sites 1 and 2, electron densities for three out of four saccharide units were seen. Site 4 did not recognize this saccharide and in site 5 only density for L-fucose was detected. Both protein subunits show a similar binding mode considering the identity of the ligand bound in the particular binding site (Table 3). In chain *B* some saccharide units in sites 1, 2 and 6 are stabilized by crystal contacts, as well as in site 3 of chain *A*.

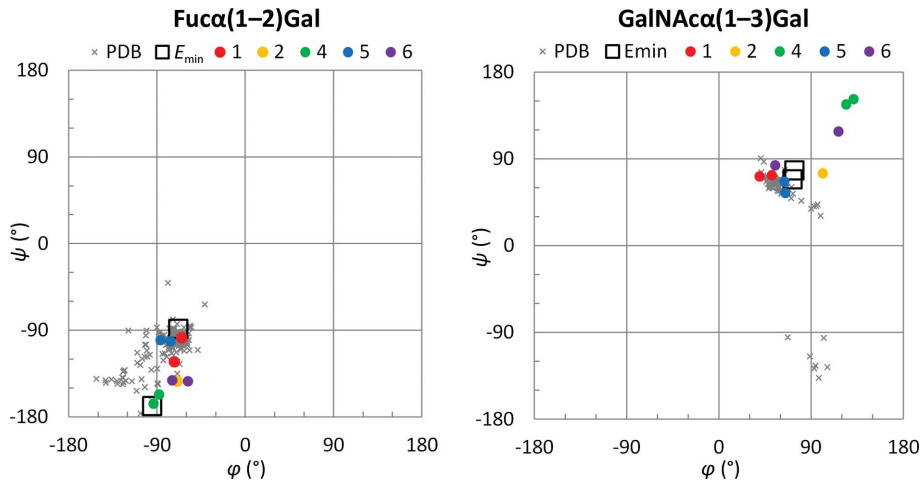

Figure 5
Sugar Ramachandran plots for the BGA epitope in the AFL complex. Ligands in each binding site are shown in different colours. The conformation of the theoretical energetic minimum (Imberty *et al.*, 1995) is shown as empty squares. Values for the particular sugar linkage derived from PDB-deposited structures using the *GlyTorsion* program are shown as grey crosses.

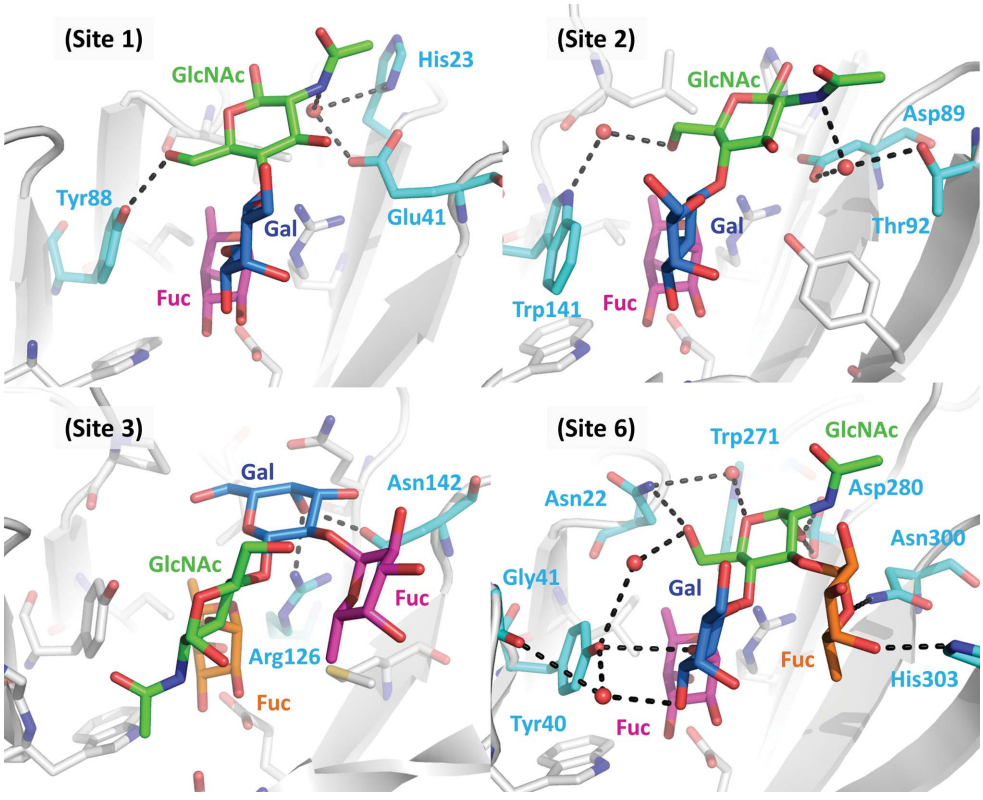

Figure 6
Le^{Y} oligosaccharides bound in AFL chain *A* sites 1, 2, 3 and 6. Colour code: α(1–2)-linked Fuc, magenta, α(1–3)-linked Fuc, orange; Gal, blue; GlcNAc, green; amino acids stabilizing saccharide units other than terminal fucose, cyan. Bridging water are shown as red spheres and hydrogen bonds are shown as black dashed lines.

Binding sites 1, 2 and 6 of both chains preferentially recognize α-1,2-linked L-fucose (Fig. 6), as is strongly supported by clear electron density for the second saccharide unit corresponding to Gal (Supplementary Fig. S7*d*). Less resolved density for the third saccharide unit in sites 1 and 2 of chain *A* suggests higher flexibility of the GlcNAc moiety. However, the positive residual density corresponding to L-fucose α(1–3)-linked to GlcNAc (Supplementary Fig. S7*d*) reveals the orientation of the GlcNAc unit, even though it does not allow assignment of the second Fuc unit. Additional interactions between the oligosaccharide and the protein were observed. The GlcNAc unit may be stabilized by Tyr88 and, through water bridges, by His23 and Glu41 in site 1 of chain *A*. In the case of site 6 of chain *A*, the O6 of the GlcNAc unit interacts with Asn22 ND2, two additional water bridges link GlcNAc to Trp271 and Tyr40 and one water bridge links O3 of the Gal unit to Tyr40 and Gly41 (Fig. 6*d*). The α-anomeric form of the O1 of GlcNAc establishes hydrogen bonds to Asp280 OD2 in site 6 of chain *A*. However, the β-anomer is usually present in biological oligosaccharides, so these interactions probably do not occur in nature.

In site 3 of both chains, the α(1–3)-linked fucose is bound (Fig. 6*c*). The Gal unit is coordinated by the Arg126 and Asn142 residues, while GlcNAc forms one weak hydrogen bond to Tyr192 in chain *B*. In site 5 only L-fucose could be assigned, while in site 4 no saccharide was found and the site is occupied by a glycerol molecule, which was used as a cryoprotecting agent.

Looking more closely at the conformation of the Lewis Y tetrasaccharide upon binding, distortion of the angles between the bound fucose and the second saccharide unit can be observed when compared with the calculated ideal values (Imberty *et al.*, 1995; Fig. 7). The rest of the saccharide tends to adopt the conformation of the minimal energy state.

4. Discussion

The biological role of fungal lectins has been the subject of debate for many years. It has been proposed that one of their key roles is in interaction with the environment, such as with the saccharides in organic matter. The pathogenic fungi may use them to interact with host tissues, which is the first step in infection.

In this paper, we investigated the relationship between the structure and the binding properties of the recently described fucose-specific lectin AFL from *A. fumigatus*. Several fungal or bacterial homologues of this protein have been described to date (Audfray *et al.*, 2011; Kostlánová *et al.*, 2005; Matsumura *et al.*, 2007), including the closely related AOL from *A. oryzae* (Ishida *et al.*, 2002) and the well known AAL from *A. aurantia* (Wimmerova *et al.*, 2003). AFL was chosen mainly for its probable role in the pathogenicity of *A. fumigatus*, which is an important opportunistic pathogen causing allergies, broncho-pulmonary aspergillosis and aspergilloma (Dagenais & Keller, 2009; Latgé, 1999).

We have demonstrated that despite the similarities between AFL and AAL, there are some interesting differences between them. Although both proteins contain tandem repeats, enabling the formation of six-bladed β-barrels in which the binding sites are located in between adjacent blades, clear differences appear in the dimer interface. The molecules of AFL are shifted with respect to the dimer of AAL, such that the central tunnels are almost aligned in AFL. This results in a larger monomer–monomer interface area (988 Å^2 in AAL and 1104 Å^2 in AFL), which implies greater dimer stability for AFL. The residues forming the intermonomer hydrogen bonds are also different, where the number of hydrogen bonds is higher in the AFL dimer.

In contrast to AAL with five binding sites (Wimmerova *et al.*, 2003), AFL possesses six binding sites, all of which are able to bind L-fucose and related saccharides. The amino acids that play a role in ligand binding are not strictly conserved in these lectins. Considering the four amino acids directly involved in Fuc binding (through hydrogen bonds or CH–π interaction), AAL sites vary only in the stacking amino acid, which can be either Trp or Tyr. Additional differences occur in AFL, including the replacement of Glu with Gln, the involvement of the main chain in the binding and the employment of water molecules to stabilize the interaction. These binding modes have not been observed in other lectins from the AAL family.

Analysis of the complexes between AFL and various ligands further confirmed the non-equivalency of its binding sites. While α-methylselenofucoside was present in the six binding sites (Houser *et al.*, 2013), L-Gal was only detected in four of them. Binding of L-Gal requires the presence of a glutamate residue to interact with O3 and O4 of the saccharide. Sites 4 and 5, where L-Gal could not bind, have Gln at this position, but they also present an unfavourable orientation of Tyr168 and Phe274, respectively, which would lead to steric conflict with O6 of L-Gal. This may correlate with the inability to fit SPR data using a two-site model. Therefore, these sites may be more specific for the α,L-fucosylated epitope than the other sites. Similarly, only some binding sites are occupied in the complex with βMeFuc. Even though the absence of β-linked fucose can be explained by steric

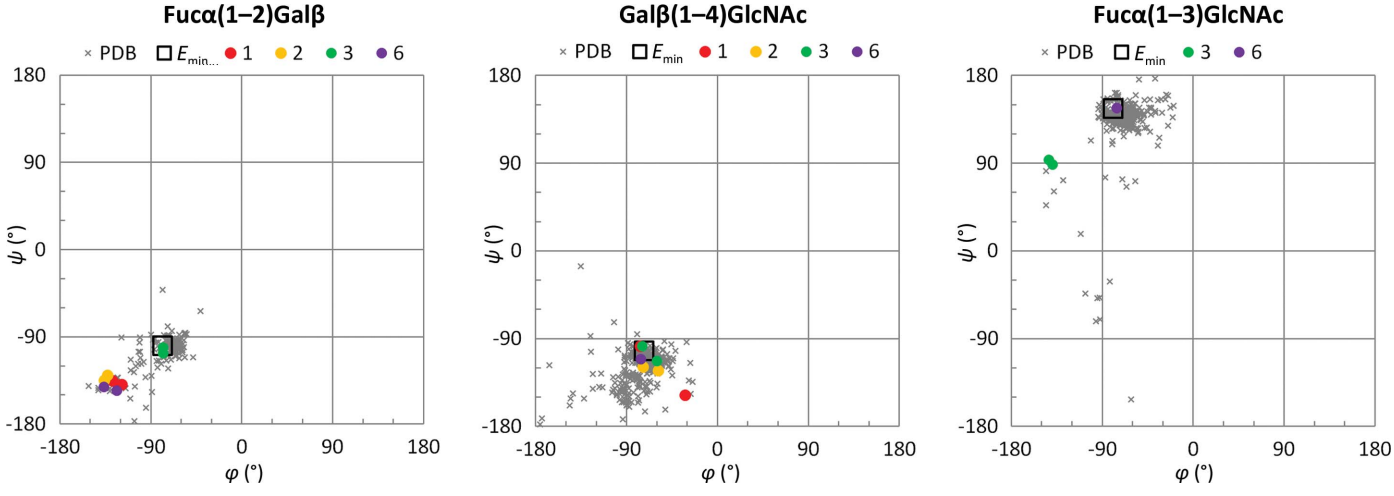

Figure 7
Sugar Ramachandran plots for the Lewis Y epitope in the AFL complex. Ligands in each binding site are shown in different colours. The conformation of the theoretical energetic minimum (Imberty *et al.*, 1995) is shown as empty squares. Values for the particular sugar linkage derived from PDB-deposited structures using the *GlyTorsion* program are shown as grey crosses.

hindrance, it is noteworthy that only sites with a stacking Tyr residue (sites 1, 3 and 6) are able to accommodate this ligand (Table 3). The only exception is site 5 in chain *C*, where the ligand is stabilized owing to crystal packing. This nicely corresponds to the SPR data, where the one-binding-site model was more suitable for the AFL–βMeFuc interaction. The lower affinity of the interaction is probably owing to the fact that stacking with Tyr residues is not as efficient as with Trp residues, as reported previously for the homologous lectin RSL from *Ralstonia solanacearum* (Wimmerová *et al.*, 2012).

The structure of the AFL–Le^Y complex revealed an interesting binding pattern in which sites 1, 2 and 6 predominantly bind the α(1–2)-linked fucose, while site 3 recognizes the α(1–3)-linked fucose. Site 5 probably binds both fucoses and site 4 is not able to accommodate the whole tetrasaccharide. This clearly demonstrates a high variability among AFL binding sites. To further decipher the preference of each binding site, we crystallized AFL with a mixture of disaccharides where Fuc is linked to the other saccharide through various linkages. All binding sites were occupied by a ligand, but only three of them preferred one particular disaccharide from the mixture, *i.e.* αFuc(1–4)GlcNAc, which is a natural epitope in plants (Fitchette-Lainé *et al.*, 1997). This preference could be explained by small differences in the binding of the ligand, where the fucoside part is crucial while the identity of the second saccharide only marginally affects the binding. Since the complexes were co-crystallized, the observed differences are probably not caused by packing but are owing to the amino-acid composition of the binding sites. In the complex with the human blood group A trisaccharide, the ligand is recognized by each binding site, but a more detailed view reveals the flexibility of the epitope. The creation of additional hydrogen bonds between the protein and the Gal or GalNAc part of the saccharide can change the torsion angles of the oligosaccharide, as can intermonomeric interactions within the crystal. Generally, AFL–sugar binding in a particular site is limited only to large epitopes or for ligands with a directly modified fucose, while α-fucosylated disaccharides and trisaccharides are recognized by all of the sites.

Several methods are commonly used to determine lectin binding affinities. Here, we demonstrated that the surface plasmon resonance method is suitable for AFL, but still has some disadvantages. AFL remains active upon immobilization and the response to binding partners is clear and dose-dependent. For low-affinity ligands the change in SPR signal is too weak, but Fuc and its derivatives were suitable analytes. The data were much more accurately fitted using the two-site binding model, showing the presence of non-equivalent binding sites. It was reported for the structurally homologous protein RSL that the stacking interaction between the saccharide unit (L-fucose) and the aromatic side chain (Trp) is crucial for high-affinity binding (Wimmerová *et al.*, 2012). The substitution of the stacking Trp residue by Phe resulted in a tenfold decrease in RSL affinity. With AFL, two sets of binding sites can be distinguished, one containing Tyr and the other containing Trp. This may correlate with the proposed two-site binding model suggested by SPR. The values of K_d are in the micromolar range for all ligands tested. This is also true for the homologous AAL (Wimmerova *et al.*, 2003) and AOL (Matsumura *et al.*, 2009). However, no significance of the existence of the high-affinity binding site in AFL was observed. The marginal difference in K_d values with respect to various fucosylated disaccharides may be caused by only infrequent interactions of the second saccharide and the AFL side chains. Comparing the previous hemagglutination data (Houser *et al.*, 2013) with the SPR results, the minimal inhibitory concentrations correlate nicely with the K_d values for the low-affinity binding sites, as expected, except for the case of αMeFuc. For the interaction with βMeFuc, the one-site model was proposed with the binding affinity being lower than in the case of αMeFuc. This may correspond to the presence of βMeFuc mainly in the Tyr-containing binding sites observed in the case of the AFL–βMeFuc complex structure. Three binding sites of both types seem to be more specific for αFuc(1–4)GlcNAc than for the other disaccharides tested, based on the crystal structure. As SPR detected αFuc(1–3)GlcNAc being bound with similar strength, both ligands are probably bound in sites where only fucose was assigned. Also, the binding might differ slightly under SPR and crystallization conditions. Of all the oligosaccharides tested, the Lewis Y tetrasaccharide was the highest affinity ligand overall. This corresponds to our previous findings using a glycan array (Houser *et al.*, 2013).

It can be concluded that AFL evolves into a multispecific lectin that is able to recognize Fuc in all possible linkages. These could be found not only in decomposed plant matter in soil, which is the natural environment for *A. fumigatus*, but also in various epitopes on human tissues. Hence, AFL may help *Aspergillus* to invade human hosts through various tissues, especially the lungs, as is most prevalent. Taking all of our findings together, AFL displays high variability in binding specificity while using a common binding motif. The similarity to the AAL lectin from *A. aurantia* is obvious, yet the differences in the number of binding sites, their specificity and affinity are interesting. Combining our results with previous work on AFL structural homologues (Audfray *et al.*, 2011; Kostlánová *et al.*, 2005; Matsumura *et al.*, 2007; Romano *et al.*, 2011; Wimmerova *et al.*, 2003) may help to understand the rules used by AAL family proteins in ligand recognition. In addition, as AFL is a potential virulence factor of *A. fumigatus*, it might be an interesting drug target. Therefore, the finding of binding-site non-equivalency is crucial for meaningful inhibitor-development and treatment strategies.

Acknowledgements

We wish to acknowledge the European Synchrotron Radiation Facility in Grenoble for access to beamline ID23-1 and ID23-2 and the Helmholtz-Zentrum Berlin for access to BESSY II beamline 14.1 and 14.2. We would like to thank to Ben Watson-Jones for language correction. The research leading to these results received financial support from the European Union under the Seventh Framework Programme by the CEITEC (CZ.1.05/1.1.00/02.0068) project from the European Regional Development Fund, SYLICA (Contract No. 286154

under the 'Capacities' specific programme), the Czech Ministry of Education (LH13055) and the Czech Science Foundation (GA13-25401S). This work was further supported by CNRS, France, the FINOVI foundation and the French Cystic Fibrosis Association Vaincre la Mucoviscidose.

References

Amano, K., Fujihashi, M., Ando, A., Miki, K. & Nagata, Y. (2004). *Biosci. Biotechnol. Biochem.* **68**, 841–847.
Audfray, A., Claudinon, J., Abounit, S., Ruvoen-Clouet, N., Larson, G., Smith, D. F., Wimmerova, M., Le Pendu, J., Romer, W., Varrot, A. & Imberty, A. (2011). *J. Biol. Chem.* **287**, 4335–4347.
Battye, T. G. G., Kontogiannis, L., Johnson, O., Powell, H. R. & Leslie, A. G. W. (2011). *Acta Cryst.* D**67**, 271–281.
Becker, D. J. & Lowe, J. B. (2003). *Glycobiology*, **13**, 41R–53R.
Chen, V. B., Arendall, W. B., Headd, J. J., Keedy, D. A., Immormino, R. M., Kapral, G. J., Murray, L. W., Richardson, J. S. & Richardson, D. C. (2010). *Acta Cryst.* D**66**, 12–21.
Dagenais, T. R. T. & Keller, N. P. (2009). *Clin. Microbiol. Rev.* **22**, 447–465.
Emsley, P., Lohkamp, B., Scott, W. G. & Cowtan, K. (2010). *Acta Cryst.* D**66**, 486–501.
Fitchette-Lainé, A.-C., Gomord, V., Cabanes, M., Michalski, J.-C., Saint Macary, M., Foucher, B., Cavelier, B., Hawes, C., Lerouge, P. & Faye, L. (1997). *Plant J.* **12**, 1411–1417.
Fujihashi, M., Peapus, D. H., Kamiya, N., Nagata, Y. & Miki, K. (2003). *Biochemistry*, **42**, 11093–11099.
Galimberti, R., Torre, A. C., Baztán, M. C. & Rodriguez-Chiappetta, F. (2012). *Clin. Dermatol.* **30**, 633–650.
Houser, J., Komarek, J., Kostlanova, N., Cioci, G., Varrot, A., Kerr, S. C., Lahmann, M., Balloy, V., Fahy, J. V., Chignard, M., Imberty, A. & Wimmerova, M. (2013). *PLoS One*, **8**, e83077.
Imberty, A., Mikros, E., Koca, J., Mollicone, R., Oriol, R. & Pérez, S. (1995). *Glycoconjug. J.* **12**, 331–349.
Imberty, A. & Varrot, A. (2008). *Curr. Opin. Struct. Biol.* **18**, 567–576.
Ishida, H., Moritani, T., Hata, Y., Kawato, A., Suginami, K., Abe, Y. & Imayasu, S. (2002). *Biosci. Biotechnol. Biochem.* **66**, 1002–1008.
Kabsch, W. (2010). *Acta Cryst.* D**66**, 125–132.
Kochibe, N. & Furukawa, K. (1980). *Biochemistry*, **19**, 2841–2846.
Kostlánová, N., Mitchell, E. P., Lortat-Jacob, H., Oscarson, S., Lahmann, M., Gilboa-Garber, N., Chambat, G., Wimmerová, M. & Imberty, A. (2005). *J. Biol. Chem.* **280**, 27839–27849.
Kuboi, S., Ishimaru, T., Tamada, S., Bernard, E. M., Kuboi, S., Perlin, D. S. & Armstrong, D. (2013). *J. Infect. Chemother.* **19**, 1021–1028.
Kwon-Chung, K. J. & Sugui, J. A. (2013). *PLoS Pathog.* **9**, e1003743.
Latgé, J.-P. (1999). *Clin. Microbiol. Rev.* **12**, 310–350.
Leslie, A. G. W. & Powell, H. R. (2007). *Evolving Methods for Macromolecular Crystallography*, edited by R. J. Read & J. L. Sussman, pp. 41–51. Dordrecht: Springer.
Matsumura, K., Higashida, K., Hata, Y., Kominami, J., Nakamura-Tsuruta, S. & Hirabayashi, J. (2009). *Anal. Biochem.* **386**, 217–221.
Matsumura, K., Higashida, K., Ishida, H., Hata, Y., Yamamoto, K., Shigeta, M., Mizuno-Horikawa, Y., Wang, X., Miyoshi, E., Gu, J. & Taniguchi, N. (2007). *J. Biol. Chem.* **282**, 15700–15708.
McCoy, A. J., Grosse-Kunstleve, R. W., Adams, P. D., Winn, M. D., Storoni, L. C. & Read, R. J. (2007). *J. Appl. Cryst.* **40**, 658–674.
Mechref, Y. & Novotny, M. V. (2002). *Chem. Rev.* **102**, 321–370.
Meisen, I., Mormann, M. & Müthing, J. (2011). *Biochim. Biophys. Acta*, **1811**, 875–896.
Mueller, U., Darowski, N., Fuchs, M. R., Förster, R., Hellmig, M., Paithankar, K. S., Pühringer, S., Steffien, M., Zocher, G. & Weiss, M. S. (2012). *J. Synchrotron Rad.* **19**, 442–449.
Murshudov, G. N., Skubák, P., Lebedev, A. A., Pannu, N. S., Steiner, R. A., Nicholls, R. A., Winn, M. D., Long, F. & Vagin, A. A. (2011). *Acta Cryst.* D**67**, 355–367.
Nurizzo, D., Mairs, T., Guijarro, M., Rey, V., Meyer, J., Fajardo, P., Chavanne, J., Biasci, J.-C., McSweeney, S. & Mitchell, E. (2006). *J. Synchrotron Rad.* **13**, 227–238.
Olausson, J., Aström, E., Jonsson, B. H., Tibell, L. A. & Påhlsson, P. (2011). *Glycobiology*, **21**, 34–44.
Olausson, J., Tibell, L., Jonsson, B. H. & Påhlsson, P. (2008). *Glycoconj. J.* **25**, 753–762.
Romano, P. R., Mackay, A., Vong, M., deSa, J., Lamontagne, A., Comunale, M. A., Hafner, J., Block, T., Lec, R. & Mehta, A. (2011). *Biochem. Biophys. Res. Commun.* **414**, 84–89.
Schuck, P. (2000). *Biophys. J.* **78**, 1606–1619.
Tiralongo, J., Wohlschlager, T., Tiralongo, E. & Kiefel, M. J. (2009). *Microbiology*, **155**, 3100–3109.
Tissot, B., North, S. J., Ceroni, A., Pang, P.-C., Panico, M., Rosati, F., Capone, A., Haslam, S. M., Dell, A. & Morris, H. R. (2009). *FEBS Lett.* **583**, 1728–1735.
Vagin, A. & Teplyakov, A. (2010). *Acta Cryst.* D**66**, 22–25.
Wimmerová, M., Kozmon, S., Nečasová, I., Mishra, S. K., Komárek, J. & Koča, J. (2012). *PLoS One*, **7**, e46032.
Wimmerova, M., Mitchell, E., Sanchez, J. F., Gautier, C. & Imberty, A. (2003). *J. Biol. Chem.* **278**, 27059–27067.
Winn, M. D. *et al.* (2011). *Acta Cryst.* D**67**, 235–242.